

Automatic delineation of the inner thoracic region in non-contrast CT data

D.R. Chittajallu, P. Balanca, and I.A. Kakadiaris, *Senior Member, IEEE*

Abstract—The inner thoracic region consists of several important anatomical structures and an accurate delineation of this region is an essential step for various biomedical image analysis applications. In this paper, we present a fully automatic graph-based method for the delineation of the inner thoracic region in non-contrast cardiac CT data. In particular, we reformulate the problem of delineating the inner thoracic region as an optimal surface segmentation problem, the solution to which is obtained by computing the minimum-cost closed set in a node-weighted directed graph. Comparing the results obtained using our method with manual segmentations performed by an expert on non-contrast cardiac CT scans of 20 randomly selected patients indicated an overlap of $99.1 \pm 0.2\%$.

I. INTRODUCTION

The inner thoracic region is the region enclosed within the inner thoracic wall, and contains several important anatomical structures (e.g., heart, lungs, coronary arteries). An accurate delineation of this region is an essential step for various biomedical image analysis applications [1]–[3].

The overall goal of this work is to improve pre-clinical diagnosis and risk prediction of cardiovascular disease (CVD) based on information (e.g., coronary artery calcium, pericardial fat volume) automatically extracted from non-contrast CT scans of the thoracic region. Prior to the extraction of such high-level information, the segmentation of the heart and other neighboring structures enclosed within the inner thoracic region is essential. An algorithm that is capable of delineating the inner thoracic region accurately can be used to obtain a good region of interest for these segmentation problems. To the best of our knowledge, no prior attempts were made to develop such an algorithm.

In this paper, we present a fully automatic graph-based method for the delineation of the inner thoracic region in non-contrast cardiac CT data. In particular, we reformulate the problem as an optimal surface segmentation problem, wherein the desired optimal surface corresponds to the inner thoracic wall. Recently, Li *et al.* [4] proposed an efficient polynomial-time method for globally optimal surface segmentation in volumetric images. We adopt this method to solve our surface segmentation problem. However, note that their method is only capable of detecting terrain-like surfaces. Since the inner thoracic wall is not a terrain-like surface, their method cannot be directly applied to obtain a solution to our problem. Hence, we transform the given volumetric image such that the desired optimal surface

corresponding to the inner thoracic wall can be represented as a terrain-like surface. Specifically, our method consists of two stages. In the first stage, we take advantage of the fact that the inner thoracic wall has a cylinder-like shape and transform the given volumetric image using a cylindrical coordinate transform centered about a point inside the inner thoracic wall. We then use the surface segmentation algorithm proposed in [4] to obtain a segmentation of the inner thoracic wall. However, this segmentation is not sufficiently accurate due to a set of issues related to the cylindrical coordinate transform which we will discuss later. In order to address this problem, we refine this segmentation in the second stage. Specifically, we compute a narrow band around the segmentation obtained in the first stage and recompute the desired optimal surface within this narrow band. We evaluated the performance of the proposed method by comparing the results obtained with manual segmentations performed by an expert. This work should be viewed in the context of graph-theoretic methods for medical image segmentation [4]–[6].

The rest of the paper is organized as follows: In Section II, we provide a detailed description of the proposed method for automatic delineation of the inner thoracic region. In Section III, we present the results obtained using the proposed method and compare them with manual segmentations performed by an expert. Finally, in Section IV, we present our conclusions.

II. METHODS

In this section, we provide a detailed description of our method for automatic delineation of the inner thoracic region in non-contrast cardiac CT data. A brief outline of the proposed method is given below:

Algorithm *Inner thoracic region segmentation*

1. **Stage 1:** Transform the given volumetric image using a cylindrical coordinate transform and compute the optimal surface (Sec. II-B).
2. **Stage 2:** Recompute the optimal surface within a narrow band around the initial segmentation obtained in stage 1 (Sec. II-C).

A. *Optimal surface segmentation method (OSS)*

In this section, we present a brief review of the method proposed by Li *et al.* [4] for optimal single surface segmentation. The solution to the optimal surface segmentation problem is obtained by computing the minimum-cost closed set in a node-weighted directed graph. The key innovation of

All authors are with the Computational Biomedicine Lab, Depts. of Computer Science, Elec. & Comp. Engineering, and Biomedical Engineering, Univ. of Houston, Houston, TX, USA

this method resides in the construction of the node-weighted directed graph that allows the transformation of the optimal surface segmentation problem into the problem of computing a minimum-cost closed set.

Consider a directed graph $G = \langle V, E \rangle$ where V is the set of vertices or nodes and E is the set of directed edges. A closed set of the digraph G is defined as a set of vertices $A \subset V$ such that if $v \in A$ and $(v, u) \in E$ then $u \in A$ (i.e., if a vertex v is in the closed set then all its successors are also in the closed set). Without loss of generality, let C be the cost function that associates each vertex $v \in V$ with a real number $C(v)$ which we refer to as the weight or cost of vertex v . Also, let \mathbb{A} be the set of all possible non-empty closed sets of the digraph G . The cost of a closed set $A \in \mathbb{A}$ is defined as the sum of costs of all the nodes belonging to the closed set A . The minimum-cost closed set problem is then to search for a closed set $A^* \in \mathbb{A}$ with minimum cost. Formally, the *minimum-cost closed set problem* can be stated as: $A^* = \arg \min_{A \in \mathbb{A}} \sum_{v \in A} C(v)$. The minimum-cost closed set problem can be solved in polynomial time by computing the s-t mincut in a derived arc-weighted directed graph [6], [7].

A volumetric image I can be viewed as a 3D matrix $I(x, y, z)$. The desired optimal surface in I is assumed to be terrain-like and oriented as shown in Fig. 1(a). Let N_x , N_y and N_z denote the size of the image I in x -, y - and z -dimensions, respectively. A feasible surface S in I is defined by a function $S : (x, y) \rightarrow S(x, y)$, where $x \in X = \{0, \dots, N_x - 1\}$, $y \in Y = \{0, \dots, N_y - 1\}$ and $S(x, y) \in Z = \{0, \dots, N_z - 1\}$. Note that any feasible surface intersects with exactly one voxel of each column of voxels parallel to the z -axis, and the entire surface consists of exactly $N_x \times N_y$ voxels. The feasibility of a surface is further constrained by application-specific smoothing constraints, enforced by two parameters, Δ_x and Δ_y , that are used to define the smoothness constraint along x - and y -directions, respectively. Specifically, if (x, y, z) and $(x+1, y, z')$ are two voxels on a feasible surface, then $|z - z'| \leq \Delta_x$. Similarly, if (x, y, z) and $(x, y+1, z')$ are two voxels on a feasible surface, then $|z - z'| \leq \Delta_y$. Smaller values of Δ_x and Δ_y enforce stronger smoothing constraints on a feasible surface.

Let $c : (x, y, z) \rightarrow c(x, y, z)$ be a cost function that assigns a cost $c(x, y, z)$ to each voxel (x, y, z) in the image I . The cost $c(x, y, z)$ is an arbitrary real number that is inversely related to the likelihood that the desired surface contains the voxel (x, y, z) . The cost of a feasible surface in I is then equal to the sum of the costs of all the voxels belonging to the surface, and the optimal surface segmentation problem is to search for a feasible surface S^* with the minimum cost among the set of all feasible surfaces \mathbb{S} definable in the image I . Formally, the *optimal surface segmentation problem* can be stated as: $S^* = \arg \min_{S \in \mathbb{S}} \sum_x \sum_y c(x, y, S(x, y))$.

A node-weighted directed graph $G = \langle V, E \rangle$ is constructed to obtain a solution to the above stated optimal surface segmentation problem as follows. Every voxel $(x, y, z) \in I$

is associated with a vertex $V(x, y, z)$ in the graph G . The cost or weight $w(x, y, z)$ assigned to the vertex $V(x, y, z)$ is defined as follows:

$$w(x, y, z) = \begin{cases} c(x, y, z) & \text{if } z = 0 \\ c(x, y, z) - c(x, y, z - 1) & \text{otherwise} \end{cases} \quad (1)$$

For each (x, y) pair in the image I such that $x \in X$ and $y \in Y$, we refer to the vertex-subset $\{V(x, y, z) | \forall z \in Z\}$ as the (x, y) -column of G and denote it by $Col(x, y)$. Two (x, y) -columns are considered to be adjacent if their corresponding (x, y) coordinates are neighbors under a given neighborhood system. For the purposes of this paper, we assume a 4-neighborhood setting. In this case, the column $Col(x, y)$ is adjacent to $Col(x + 1, y)$, $Col(x - 1, y)$, $Col(x, y + 1)$, and $Col(x, y - 1)$. The edge set E of the digraph G consists of two types of edges, *intra-column* edges and *inter-column* edges, which are defined as follows [4]:

- *intra-column edges*: Within each column $Col(x, y)$, every vertex $V(x, y, z)$, $z > 0$ has a directed edge to the vertex $V(x, y, z - 1)$.
- *inter-column edges*: Without loss of generality, consider two adjacent columns $Col(x, y)$, $x < N_x - 1$, and $Col(x + 1, y)$ along the x -direction. Each vertex $V(x, y, z) \in Col(x, y)$ is connected by a directed edge to the vertex $V(x + 1, y, \max(0, z - \Delta_x)) \in Col(x + 1, y)$. Also, a directed edge is established from the vertex $V(x + 1, y, z) \in Col(x + 1, y)$ to the vertex $V(x, y, \max(0, z - \Delta_x)) \in Col(x, y)$. Similar construction is performed for two adjacent columns along the y -direction. Figure 1(b) depicts the edges between the two adjacent columns along the x -direction. Note that these inter-column arcs are responsible for guaranteeing that if a voxel (x, y, z) is on a feasible surface S , then its neighboring voxel $(x + 1, y, z')$ on the surface S along the x -direction satisfies the required smoothness constraint, $|z - z'| \leq \Delta_x$. The same holds for two adjacent columns along the y -direction.

With the above-described graph-construction, it is easy to show that the minimum-cost closed set of the graph G solves the optimal surface segmentation problem.

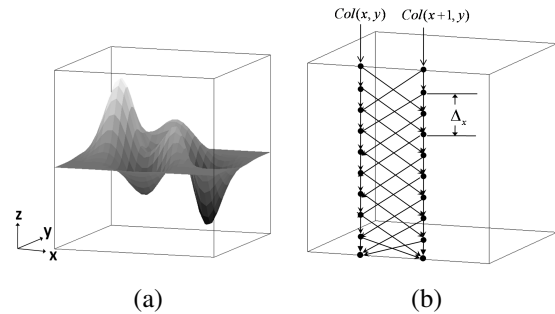


Fig. 1. Optimal surface segmentation problem. (a) Orientation of the optimal surface. (b) Two adjacent columns along the x -direction of the constructed node-weighted digraph.

B. Stage 1: Initial segmentation of the thoracic wall using a cylindrical coordinate transform

We reformulate the problem of delineating the inner thoracic region as an optimal surface segmentation problem wherein the desired optimal surface corresponds to the inner thoracic wall. We use OSS (see Sec. II-A) to solve the optimal surface segmentation problem. However, in order to use OSS, the desired optimal surface should be terrain-like, as depicted in Fig. 1(a), which is not the case for our problem. Hence, we transform the given volumetric image such that the desired optimal surface corresponding to the inner thoracic wall can be represented as a terrain-like surface. Specifically, we take advantage of the fact that the inner thoracic wall has a cylinder-like shape and transform the given volumetric image using a cylindrical coordinate transform (CCT) centered about a point inside the inner thoracic wall. We will refer to this transformed image space as the CCT space.

The key to achieving a good segmentation result to any given problem using OSS resides in the design of a good cost function $c(x, y, z)$ (Eq. 1). From prior knowledge about the location of the inner thoracic wall, we require the optimal surface to pass through the set W_{LB} of voxels along the inner walls of the ribcage and the outer walls of the lungs. In order to incorporate this prior knowledge, we first perform a rough segmentation of the lungs and the ribcage using simple thresholding and connected component analysis. Figures 2(a) and (b) depict an overlay of the lung and ribcage masks in the original and CCT space, respectively. We can then easily identify the set W_{LB} of voxels in the CCT space as the “bottom-most” voxels of the lungs and the “top-most” voxels of the ribcage in each (x, y) -column. A very low cost must be assigned to these voxels in order to impose a hard constraint that the computed optimal surface passes through these voxels. In the case where none of the voxels in an (x, y) -column belong to the set W_{LB} , which occurs at the interface between the mediastinum and inner-thoracic wall, we require the optimal surface to pass through the nearest fat-to-muscle transition. This can be captured by a positive y -gradient in the CCT space. Based on the above discussion, we design the cost function as follows:

$$c(x, y, z) = \begin{cases} c_{min} & \text{if } (x, y, z) \in W_{LB} \\ -g_y(x, y, z) & \text{otherwise} \end{cases} \quad (2)$$

where g_y denotes the y -gradient in the CCT space and $c_{min} < \min(g_y)$. Figure 2(c) depicts the cost function on a slice in the CCT space. Given this cost function, we then use OSS to compute the globally optimal surface. Figures 2(d) and (e) depict the segmentation result obtained in the CCT space and the original image space, respectively.

The quality of the segmentation result obtained in this stage depends on the angular and radial resolution of the CCT transform. The finer the angular and radial resolution, the better would be the segmentation result. However, the finer the resolution, the bigger would be the size of the graph and the higher would be the memory requirements and

the computational time needed to solve the optimal surface segmentation problem. In order to address this issue, we compute the optimal surface with a coarser angular and radial resolution in this stage and further refine it in the second stage of our method (Sec. II-C).

C. Stage 2: Refinement of the initial segmentation within a narrow band

In this stage, we refine the initial segmentation result obtained in the first stage by recomputing the optimal surface in a narrow band around it. In order to compute the band, we first compute the minimum intensity projection of the initial segmentation result along the z -axis of the image space. We then erode and dilate this mask to define a narrow band around the initial segmentation result. Note that the band computation is performed in the original image space and the same band is used in all the axial slices of the given volumetric image. Figure 3(a) depicts the narrow band computed in an axial slice. Once the band computation is complete, we flatten the portion of the volume within this band as depicted in Figure 3(b). We then use OSS to compute the optimal surface in this new band space. Note that we use the same cost function in both stages of our method. Figure 3(c) depicts the cost function in the band space. Figures 3(d) and (e) depict the segmentation result obtained in the band space and the original image space, respectively.

III. RESULTS AND DISCUSSION

We applied our *Inner thoracic region segmentation* algorithm on non-contrast cardiac CT scans of 20 randomly selected patients. The non-contrast cardiac CT scans were acquired on an electron-beam CT (EBCT) scanner (GE Imatron). For each scan, a stack of 20-36 contiguous slices were acquired with a slice thickness of 3 mm each. The pixel sizes ranged from 0.508 mm to 0.586 mm. The accuracy of the segmentation results obtained was evaluated by measuring the degree of overlap with manual segmentation performed by an expert. The degree of overlap was estimated using the Dice similarity coefficient (DSC). Table I provides descriptive statistics of the DSC measure obtained in the first and second stages of our method. We used DSC to measure the degree of overlap in the entire volume (Total Overlap) and also within the narrow band (Band Overlap) used in the second stage of our method. As is evident from Table I, the DSC of stage 2 is significantly higher than that of stage 1. This indicates that the refinement performed in stage 2 significantly improves the segmentation performance. Figure 4 depicts 3D visualizations of the segmentation results obtained using our method on non-contrast cardiac CT scans of four randomly selected patients.

IV. CONCLUSION

In this paper, we have presented a fully automatic graph-based method for the delineation of the inner thoracic region

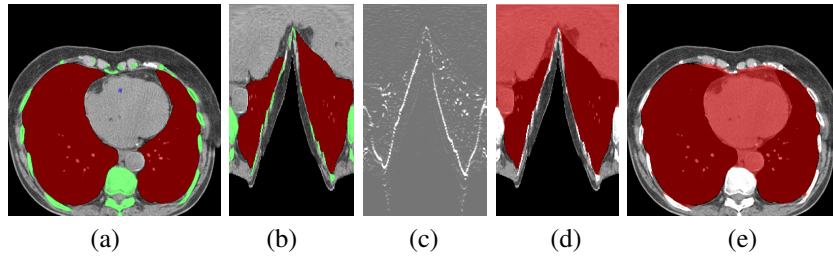


Fig. 2. Stage 1: (a,b) Overlay of the lung (red) and ribcage (green) masks in the original and CCT space, respectively. (c) Negative of the cost function used for the optimal surface segmentation problem. (d,e) Overlay of the segmentation result obtained in the CCT and original image space, respectively.

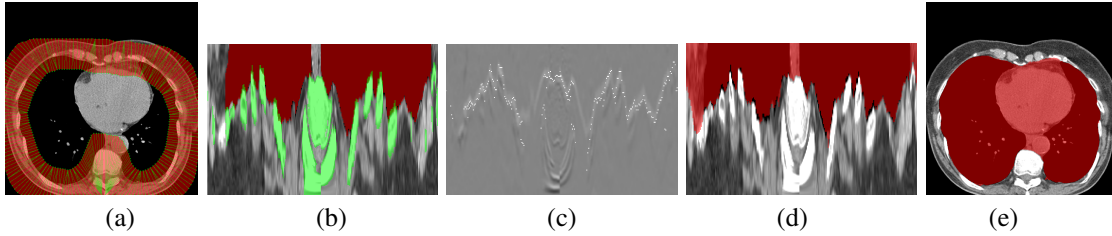


Fig. 3. Stage 2: (a) Narrow band computed around the segmentation result obtained in stage 1. (b) Band unwrapped image overlaid with the lung (red) and ribcage (green) masks. (c) Negative of the cost function used for the optimal surface segmentation problem. (d,e) Overlay of the segmentation result obtained in the band space and the original image space, respectively.

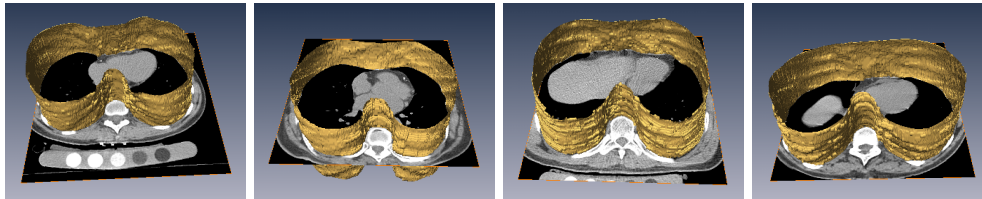


Fig. 4. 3D visualization of the segmentation result obtained using our method on non-contrast cardiac CT scans of four randomly selected patients.

TABLE I

DESCRIPTIVE STATISTICS OF THE DICE SIMILARITY COEFFICIENT (DSC) OBTAINED IN THE FIRST AND SECOND STAGES OF OUR METHOD.

	DSC (<i>mean</i> \pm <i>std</i>)	DSC Range
Total Overlap Stage 1	0.985 \pm 0.005	[0.962, 0.990]
Total Overlap Stage 2	0.991 \pm 0.002	[0.981, 0.993]
Band Overlap Stage 1	0.945 \pm 0.014	[0.910, 0.971]
Band Overlap Stage 2	0.968 \pm 0.007	[0.950, 0.981]

in non-contrast cardiac CT data with very encouraging results. The proposed method can be easily adapted for the data from other imaging modalities (e.g., CTA and MRI).

V. ACKNOWLEDGMENTS

This work was supported in part by the NIH Grant 1R21EB006829, the NSF Grants IIS-0431144, and CNS-0521527 and the UH Eckhard Pfeiffer Endowment Fund. Any opinions, findings, conclusions or recommendations expressed in this material are the authors' and may not reflect the views of the sponsors.

REFERENCES

- [1] G. Brunner, D. R. Chittajallu, U. Kurkure, and I. A. Kakadiaris, "A heart-centered coordinate system for the detection of coronary artery zones in non-contrast Computed Tomography data," in *Proc. Medical Image Computing and Computer-Assisted Intervention Workshop on*
- [2] U. Kurkure, D. R. Chittajallu, G. Brunner, R. Yalamanchili, and I. A. Kakadiaris, "Detection of coronary calcifications using supervised hierarchical classification," in *Proc. Medical Image Computing and Computer-Assisted Intervention Workshop on Computer Vision for Intravascular and Intracardiac Imaging*, New York, NY, Sep. 10 2008.
- [3] A. Bandekar, M. Naghavi, and I. A. Kakadiaris, "Automated pericardial fat quantification in CT data," in *Proc. 28th International Conference of the IEEE Engineering in Medicine and Biology Society*, New York, NY, Aug. 30 - Sep. 3 2006, pp. 932–936.
- [4] K. Li, X. Wu, D. Z. Chen, and M. Sonka, "Optimal surface segmentation in volumetric images—a graph-theoretic approach," *IEEE Transactions on Pattern Analysis and Machine Intelligence*, vol. 28, no. 1, pp. 119–134, 2006.
- [5] L. Grady, "Computing exact discrete minimal surfaces: extending and solving the shortest path problem in 3d with application to segmentation," in *Proc. IEEE Computer Society Conference on Computer Vision and Pattern Recognition*, vol. 1, June 2006, pp. 69–78.
- [6] Y. Boykov and V. Kolmogorov, "An experimental comparison of min-cut/max-flow algorithms for energy minimization in vision," *IEEE Transactions on Pattern Analysis and Machine Intelligence*, vol. 26, no. 9, pp. 1124–1137, 2004.
- [7] J.-C. Picard, "Maximal closure of a graph and applications to combinatorial problems," *Management Science*, vol. 22, no. 11, pp. 1268–1272, 1976.